

## HETEROGENEOUS WATER CONTENT IN THE LUNAR INTERIOR: INSIGHTS FROM ORBITAL DETECTION OF WATER IN PYROCLASTIC DEPOSITS AND SILICIC DOMES.

S. Li<sup>1</sup> and R. E. Milliken<sup>1</sup>, <sup>1</sup>Department of Earth, Environmental, and Planetary Sciences, Brown University, Providence, RI, 02912, [shuai\\_li@brown.edu](mailto:shuai_li@brown.edu)

**Introduction:** Constraining the distribution and abundance of water (H<sub>2</sub>O and/or OH) in the lunar interior is crucial for assessing the formation and evolution of the Moon. Hundreds parts per million (ppm) of water has been identified as of endogenous lunar origin in Apollo 15 and 17 volcanic glasses [1,2]. However, other lines of evidence suggest that the lunar interior may not have such high values of water [4-6], and assessing water variations in the lunar interior is constrained by limited sampling locations. Reflectance spectra for the 3 $\mu$ m wavelength region, remotely sensed by the Moon Mineralogy Mapper (M<sup>3</sup>), provide an alternative way to characterize lunar water at a global scale. Though such methods only probe the optical surface, hydration in some materials may result from internal processes. Constraining the volatile content of pyroclastic deposits and silicic rich domes, for example, can provide insight into volatile distribution and evolution related to magmatic processes. The goal of this work is to examine and quantify the potential indigenous water content of lunar pyroclastic deposits and silicic rich domes to provide a broader picture of magma volatile content and variations in magma degassing history on the Moon.

Water at the lunar optical surface can be sourced from solar wind implantation, impacts (asteroids/comets), and the lunar interior [4]. The water content measured in the Apollo bulk samples is ~50-60 ppm on average [4], which provides constraints for our mapping results at similar latitudes (i.e.,  $\sim \pm 30^\circ$ ) as well as potential 'background' hydration level. The maximum background water content is removed from our prior mapping results [3] to examine what may be considered 'excess' water signature at pyroclastic deposits and silicic rich domes. The 'excess' water signatures may originate from the interior.

**Methods:** We previously used M<sup>3</sup> data to map Hapke's Effective Single Particle Absorption Thickness (ESPAT) at  $\sim 2.9 \mu\text{m}$  as a linear proxy for water content [3]. Laboratory experiments and numerical simulations were used to determine specific H<sub>2</sub>O%-ESPAT trends in order to estimate water content from ESPAT. Lab spectra of basaltic glasses (synthetic and natural) and terrestrial anorthosite were measured using FTIR and ASD spectrometers in the RELAB facility at Brown University. Absolute water content of the basaltic glasses were previously measured with SIMS in [8,9] and the water content of anorthosite was determined by stepwise heating and weight loss. These samples were sieved into four particle size ranges (<45 $\mu\text{m}$ , 32-53 $\mu\text{m}$ , 63-75 $\mu\text{m}$ , and 106-125 $\mu\text{m}$ ) to determine how H<sub>2</sub>O%-ESPAT trends are affected by particle size. The FTIR reflectance spectra were scaled to the respective ASD spectra to get the absolute reflectance at  $\sim 2.9 \mu\text{m}$  (the 'water' bands), and ESPAT for each sample was calculated in the same way as for the M<sup>3</sup> data. The lab-based H<sub>2</sub>O%-ESPAT trends were also regressed and compared with simulations from radiative transfer modeling.

**Results and Discussion:** Experimental results show that H<sub>2</sub>O%=1.8·ESPAT for samples <45 $\mu\text{m}$ , regardless of composition, which we find to be consistent with simulations based on absorption coefficients measured in [10] (Fig. 1). Other particle size groups of basaltic glass also match well with the simulations (dashed lines in Fig. 1). Experiments for additional particle sizes of anorthosite are currently underway, but these H<sub>2</sub>O%-ESPAT trends are expected to match with those of basaltic glasses of similar particle size. The mean particle size of bulk Apollo soil samples is  $\sim 60\text{-}80\mu\text{m}$  [11]. If such a range is representative of the particle size of lunar regolith at all similar latitudes (i.e.,  $\sim \pm 30^\circ$ ), then

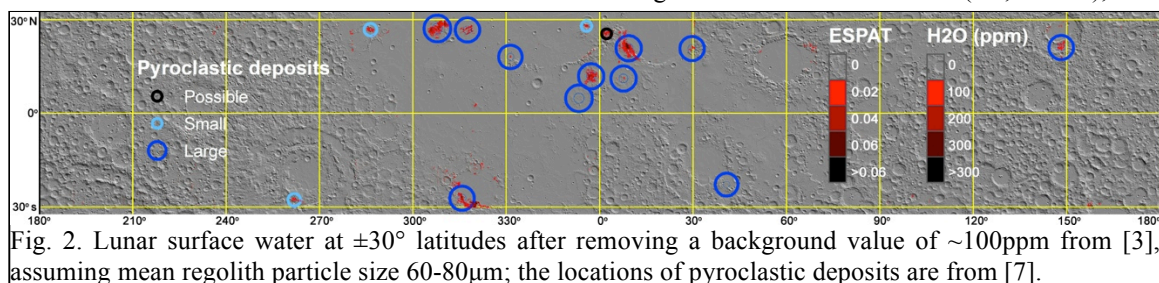


Fig. 2. Lunar surface water at  $\pm 30^\circ$  latitudes after removing a background value of  $\sim 100$  ppm from [3], assuming mean regolith particle size 60-80 $\mu\text{m}$ ; the locations of pyroclastic deposits are from [7].

our lab results suggest  $H_2O\% \approx 0.5 \cdot ESPAT$ .

The water content of lunar surface between  $\pm 30^\circ$  latitudes was derived from our mapped ESPAT using this relationship and it exhibits good agreement with the measurements from Apollo samples [3] in that the maximum 'background' water content at these latitudes is  $\sim 100$  ppm. After subtracting this background value from all pixels, Fig. 2 reveals that only pyroclastic deposits exhibit 'excess' or increased water signature.

We interpret this excess water to be associated with volcanic glass and thus sourced from the lunar interior. The average water content of all large pyroclastic deposits is plotted with their areal range in Fig. 3, and low and high Ti deposits exhibit different trends (Fig. 3). Magma eruption models can be used to estimate what volatile content would be required to generate such sizes of pyroclastic deposits [12], and analyses of Apollo volcanic glasses suggest that only  $\sim 1\%$  of volatiles from the magma sources might be water [8]. Together, these models can be used to estimate the water content of magma sources for different pyroclastic deposits and compared with the  $M^3$ -derived values.

Our estimated water contents are much less than estimates from magma eruption models (Fig. 3), and the difference may be attributed to magma degassing. Indeed, the different water loss trends between the low and high Ti deposits can be interpreted as more water in high Ti magma sources and/or faster cooling rates for high Ti deposits. However, simple diffusion modeling suggests that different cooling rates may not be able to explain all of the differences, thus source magmas for high-Ti deposits may have higher volatile content. If true, this would indicate the lunar interior (or at least sources for pyroclastic deposits) is heterogeneous in water content and that these variations can be inferred from orbital data.

Reported silicic rich domes on the Moon may be formed through fractional crystallization of magmas or ascent of silicic rich melts due to

its immiscibility and low density [13]. If there were any water in the source regions then it could have been concentrated in silicic rich melts and brought to the surface. We examined the hydration state of all possible silicic rich domes on the Moon (Fig. 4) and found that only some exhibit enhanced hydration, which could be due to: 1) more complicated cooling history compared with pyroclastic deposits; 2) increased variability in the water content of magma source regions; 3) variations in composition that affect retention of water or ambiguity in identification of these regions as being silica-rich.

**Conclusions:** We have assessed the water content at lunar pyroclastic deposits and silicic rich domes using orbital observations, supported with laboratory measurements and spectral radiative transfer models of lunar-relevant materials. Water content at  $\pm 30^\circ$  latitude shows consistency with that measured from Apollo bulk samples (soils and rocks). Excess water signature observed in all large pyroclastic deposits in this latitude zone is consistent with an endogenous origin and suggests a hydrated yet heterogeneous lunar interior. However, only some of silicic rich domes exhibit enhanced hydration, which could be due to a more complicated degassing history, different water content in the magma sources, or ambiguity in identification of their composition.

References: [1] Saal, A. E. *et al.* (2008). *Nature*, **454**. [2] Hauri, E. H. *et al.* (2011). *Science*, **333**. [3] Li, S. and Milliken, R. (2015) *LPSC*. [4] Epstein, S. and Taylor, J., HP. (1970). *GCA*, **1**. [5] Sharp, Z. D. *et al.* (2010). *Science*, **329**. [6] Elkins-Tanton, L. T. and Grove, T. L. (2011). *EPSL*, **307**. [7] Gaddis, L. R. *et al.* (2003). *Icarus*, **161**. [8] Wetzell, D. T. *et al.* (2015). *Nat Geosci*, **8**. [9] Shimizu, K. *et al.* (2015). *GCA* [10] Stolper, E. (1982). *CMP*, **81**. [11] Heiken, G. H. *et al.* (1991) Cambridge University Press. [12] Wilson, L. and Head, J. (1981). *JGR*, **86**. [13] Glotch, T. D. *et al.* (2010). *Science*, **329**.

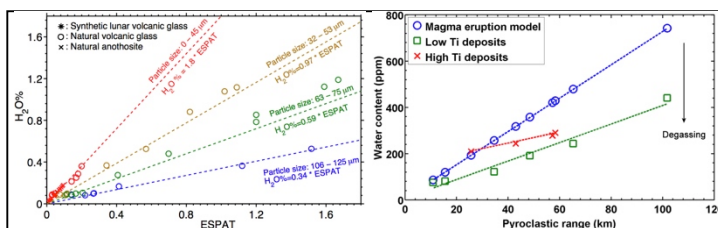


Fig. 1. Experimental results for the H<sub>2</sub>O-ESPAT trends for basaltic glasses and anorthosite.

Fig. 3. Average water contents vs. pyroclastic ranges for large pyroclastics at  $\pm 30^\circ$  latitudes.

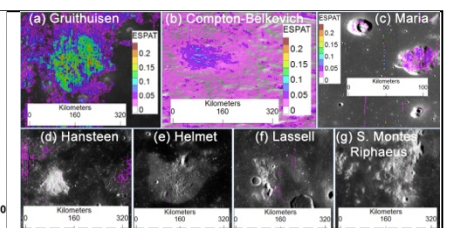


Fig. 4. Hydration status of possible silicic rich domes.